AFRL-ML-WP-TP-2006-487

DEFORMATION AND RECRYSTALLIZATION DURING THERMOMECHANICAL PROCESSING OF A NICKEL-BASE SUPERALLOY INGOT MATERIAL (POSTPRINT)

S.L. Semiatin, D.S. Weaver, R.L. Goetz, J.P. Thomas, and T.J. Turner

SEPTEMBER 2006

Approved for public release; distribution is unlimited.

STINFO COPY

MATERIALS AND MANUFACTURING DIRECTORATE
AIR FORCE RESEARCH LABORATORY
AIR FORCE MATERIEL COMMAND
WRIGHT-PATTERSON AIR FORCE BASE, OH 45433-7750

REPORT DOCUMENTATION PAGE

Form Approved
OMB No. 0704-0188

1. REPORT DATE *(DD-MM-YY)*	2. REPORT TYPE	3. DATES COVERED *(From - To)*
September 2006	Conference Paper Postprint	N/A

4. TITLE AND SUBTITLE
DEFORMATION AND RECRYSTALLIZATION DURING THERMOMECHANICAL PROCESSING OF A NICKEL-BASE SUPERALLOY INGOT MATERIAL (POSTPRINT)

5a. CONTRACT NUMBER
F33615-04-D-5235

5b. GRANT NUMBER

5c. PROGRAM ELEMENT NUMBER
N/A

6. AUTHOR(S)
D.S. Weaver, S.L. Semiatin, and T.J. Turner (AFRL/MLLMP)
R.L. Goetz (UES, Inc.)
J.P. Thomas (Universal Technology Corporation)

5d. PROJECT NUMBER
N/A

5e. TASK NUMBER
N/A

5f. WORK UNIT NUMBER
N/A

7. PERFORMING ORGANIZATION NAME(S) AND ADDRESS(ES)
UES, Inc.
4401 Dayton-Xenia Rd.
Dayton, OH 45432-1894

Universal Technology Corporation
1270 North Fairfield Road
Dayton, OH 45432

Processing Section, Metals Branch (AFRL/MLLMP)
Metals, Ceramics, and Nondestructive Evaluation Division
Materials and Manufacturing Directorate
Air Force Research Laboratory, Air Force Materiel Command
Wright-Patterson Air Force Base, OH 45433-7750

8. PERFORMING ORGANIZATION REPORT NUMBER

9. SPONSORING/MONITORING AGENCY NAME(S) AND ADDRESS(ES)
Materials and Manufacturing Directorate
Air Force Research Laboratory
Air Force Materiel Command
Wright-Patterson AFB, OH 45433-7750

10. SPONSORING/MONITORING AGENCY ACRONYM(S)
AFRL-ML-WP

11. SPONSORING/MONITORING AGENCY REPORT NUMBER(S)
AFRL-ML-WP-TP-2006-487

12. DISTRIBUTION/AVAILABILITY STATEMENT
Approved for public release; distribution is unlimited.

13. SUPPLEMENTARY NOTES
 Conference paper published in Materials Science Forum Vol. 550 (2007).
PAO Case Number: AFRL/WS 06-1595, 06 Aug 2006.

14. ABSTRACT
The deformation response and recrystallization behavior of a coarse, columnar-grain superalloy ingot material, Waspaloy, with a <100> fiber texture were established. For this purpose, isothermal hot compression tests were performed on cylindrical and doublecone samples at supersolvus temperatures under both monotonic (constant strain rate) and multi-hit conditions. Plastic flow showed a noticeable dependence on test direction relative to the columnar-grain orientation; the observed anisotropy in peak flow stress and flow softening were explained on the basis of the evolution of crystallographic texture during recrystallization. Similarly, anisotropy in dynamic recrystallization kinetics with respect to test direction was interpreted in terms of the effect of initial texture on the plastic work imposed per increment of macroscopic strain. Nevertheless, the broad kinetics for the coarse-grain, ingot material deformed under both monotonic and multi-hit conditions were comparable to those previously measured for fine-grain, wrought Waspaloy. Such an effect was attributed to the beneficial influence of the nucleation of recrystallization at both grain boundaries and carbide particles in the ingot material. In addition, a spatial non-uniformity in recrystallization was found in the ingot material and was interpreted in the context of the grain-boundary character and non-uniform strain at the grain/intragrain scale. A suite of tools being developed to model recrystallization phenomena during the breakdown of superalloy ingots is described. These tools include a mechanistic cellular automata; a mesoscale, mechanism-based model; and the crystal-plasticity finite-element method.

15. SUBJECT TERMS dynamic recrystallization, metadynamic recrystallization, grain growth, ingot breakdown, fiber texture, cellular automata, mesoscale modeling

16. SECURITY CLASSIFICATION OF:			17. LIMITATION OF ABSTRACT:	18. NUMBER OF PAGES	19a. NAME OF RESPONSIBLE PERSON (Monitor)
a. REPORT	b. ABSTRACT	c. THIS PAGE			S.L. Semiatin
Unclassified	Unclassified	Unclassified	SAR	18	19b. TELEPHONE NUMBER *(Include Area Code)* N/A

Materials Science Forum Vol. 550 (2007) pp. 129-140
online at http://www.scientific.net

Deformation and Recrystallization during Thermomechanical Processing of a Nickel-Base Superalloy Ingot Material

S.L. Semiatin[1, a], D.S. Weaver[2,b], R.L. Goetz[3,c], J.P. Thomas[4,d], and T.J. Turner[5,e]

[1,2,5]Air Force Research Laboratory, Materials and Manufacturing Directorate, AFRL/MLLM, Wright-Patterson Air Force Base, OH 45433, USA

[3]UES, Inc., 4401 Dayton-Xenia Road, Dayton, OH 45432, USA

[4]Universal Technology Corporation, 1270 N. Fairfield Road, Dayton, OH 45432, USA

[a]lee.semiatin@wpafb.af.mil, [b]donald.weaver@wpafb.af.mil, [c]robert.goetz@wpafb.af.mil, [d]jp.thomas@afmcx.net, [e]todd.turner@wpafb.af.mil

Keywords: dynamic recrystallization, metadynamic recrystallization, grain growth, ingot breakdown, fiber texture, cellular automata, mesoscale modeling.

Abstract. The deformation response and recrystallization behavior of a coarse, columnar-grain superalloy ingot material, Waspaloy, with a <100> fiber texture were established. For this purpose, isothermal hot compression tests were performed on cylindrical and double-cone samples at supersolvus temperatures under both monotonic (constant strain rate) and multi-hit conditions. Plastic flow showed a noticeable dependence on test direction relative to the columnar-grain orientation; the observed anisotropy in peak flow stress and flow softening were explained on the basis of the evolution of crystallographic texture during recrystallization. Similarly, anisotropy in dynamic recrystallization kinetics with respect to test direction was interpreted in terms of the effect of initial texture on the plastic work imposed per increment of macroscopic strain. Nevertheless, the broad kinetics for the coarse-grain, ingot material deformed under both monotonic and multi-hit conditions were comparable to those previously measured for *fine-grain*, wrought Waspaloy. Such an effect was attributed to the beneficial influence of the nucleation of recrystallization at both grain boundaries and carbide particles in the ingot material. In addition, a spatial non-uniformity in recrystallization was found in the ingot material and was interpreted in the context of the grain-boundary character and non-uniform strain at the grain/intragrain scale. A suite of tools being developed to model recrystallization phenomena during the breakdown of superalloy ingots is described. These tools include a mechanistic cellular automata; a mesoscale, mechanism-based model; and the crystal-plasticity finite-element method.

Introduction

The production of nickel-base superalloys for high-temperature applications usually comprises a powder (PM) or ingot-metallurgy (IM) approach. PM techniques are used predominately for highly-alloyed materials (e.g., Rene 88, IN-100) which are prone to segregation during solidification or exhibit poor hot workability in the cast, coarse-grain condition. Powder components are typically fabricated via a series of steps involving initial consolidation (via blind-die compaction or hot-isostatic pressing), hot extrusion, and isothermal, closed-die forging under superplastic conditions. These processing steps ensure the break-up of prior-particle boundaries and recrystallization. By contrast, the IM processing of superalloys such as 718 and Waspaloy consists of initial synthesis (via vacuum-induction melting (VIM) and remelting of ingots by vacuum arc (VAR) or electroslag (ESR) techniques), homogenization heat treatment (to eliminate microsegregation), and a series of upsetting and drawing (cogging) operations to produce a uniform, fine-grain microstructure via recrystallization of the initial coarse-grain ingot material.

The effect of hot working variables on the recrystallization of *fine-grain* wrought materials has been studied extensively [1]. On the other hand, very little work has been performed to determine the mechanisms and kinetics of microstructure evolution in production-scale cast ingots of engineering materials because of challenges related to cost and grain size. Such ingots are typically 500 to 1200 mm in diameter, 1500 to 2500 mm in length, and weigh five tons or more. In addition, a large portion of the ingot structure comprises columnar grains whose diameter is of the order of several millimeters and which bear the signature of a marked solidification texture [2]. Despite the difficulty of working with cast ingots, it may be hypothesized that microstructure evolution during the initial thermomechanical processing (TMP) of such materials may contrast sharply with the behavior of the corresponding wrought alloy. For example, Avrami fits for discontinuous dynamic recrystallization (DDRX) of wrought materials typically show a strong dependence on initial grain size [3, 4], most likely because of the fact that nucleation usually occurs at grain boundaries. For a similar reason, Avrami-type models often exhibit a dependence of recrystallization on grain *shape* through its effect on the "dimensionality" of the progression of recrystallization [5].

The objectives of the present work were to (1) develop a fundamental understanding of the mechanisms and kinetics of the processes that control microstructure evolution during ingot breakdown for a typical superalloy, Waspaloy, and (2) formulate appropriate mechanism-based models to treat such processes.

Materials and Procedures

Material. The material used in the present work was taken from the columnar-grain regions of a 508-mm-diameter, homogenized ingot of Waspaloy produced by a standard VIM/VAR approach [6]. The grains had an average diameter of ~4.8 mm and length of ~44 mm. Electron-backscatter diffraction (EBSD) analysis revealed that the columnar grains exhibited a <100> fiber texture typical of the solidification of fcc materials. Furthermore, optical metallography on polished sections revealed a distribution of coarse, largely globular, carbide particles whose size was ~10 μm and volume fraction was ~0.3 pct. The gamma-prime solvus was estimated to be 1030°C [6].

Procedures. Isothermal hot compression tests were conducted on cylindrical and double-cone samples to establish the plastic-flow and dynamic/static recrystallization behavior, respectively, of the cast-and-homogenized material. For this purpose, samples were cut such that the columnar-grain axis lay parallel, perpendicular, or 45° to the compression axis. Samples and tooling were induction preheated and upset under constant strain rate conditions either monotonically or with intermediate dwells between strain increments. The *monotonic* tests were conducted at supersolvus temperatures of 1066 or 1177°C and strain rates of 0.005 or 0.1 s^{-1} to a height reduction between 2:1 and 4:1; following compression, each sample was either water quenched immediately or allowed to undergo metadynamic recrystallization (MDRX) /grain growth for times between 30 s and 30 min. In order to simulate production cogging practices, *interrupted* tests were performed at identical test temperatures and strain rates (to a total reduction of 3:1) using dwell times of 20, 30, or 60 s between imposed strain increments of 0.15. Standard optical, SEM, and quantitative metallography techniques and electron-backscatter diffraction (EBSD) analysis were used to characterize the final microstructure (e.g., recrystallized fraction, recrystallized grain size) and texture.

The experimental observations were interpreted using both phenomenological (Avrami) methods and micro-mechanical models. The latter consisted of a cellular-automata model, a novel mesoscale simulation technique, and crystal-plasticity finite-element-method (FEM) calculations.

Results

The principal experimental results pertain to the effect of texture/test orientation on plastic flow behavior and the kinetics and mechanisms of recrystallization of the columnar-grain microstructure.

Plastic Flow Behavior. True stress-strain curves measured on axial and transverse samples showed a noticeable difference, irrespective of test temperature and strain rate (Fig. 1). In all cases, the flow curves of the *axial* samples exhibited an initial strain-hardening transient followed by near-steady-state flow (i.e., a constant flow stress). By contrast, the flow curves for the *transverse* samples showed an initial strain-hardening period, a peak stress (which was higher than that for the axial samples), and flow softening. Even though the rate of softening decreased with increasing strain, steady-state flow was not achieved even at the maximum strain imposed (~1) in the uniaxial compression tests.

The plastic-flow observations were interpreted in terms of the effect of initial texture and texture changes during hot compression. Assuming axisymmetric deformation via octahedral slip [7], the average Taylor factors (M_T) for the cast material compressed either parallel or transverse to the <100> fiber texture were 2.45 or ~3.1, respectively [8]. The ratio of these values of M (i.e., ~0.8) mirrors the relative peak stresses for axial versus transverse compression tests (Fig. 1). The development of a near-random recrystallization texture (with M ~ 2.9) during deformation provided an explanation for the observed flow-softening anisotropy. Specifically, the flow *softening* observed for the transverse samples can be ascribed to classical DDRX and its associated dislocation-annihilation process in view of the near absence of texture hardening/softening during dynamic recrystallization. On the other hand, the texture *hardening* associated with the increase in the Taylor factor (from ~2.45 to ~2.9) during the hot deformation of the axial samples counterbalanced the flow softening characterizing DDRX per se. Fig. 1 also illustrates the near convergence of the flow curves of the axial and transverse tests at large strains. The absence of true steady-state flow after a strain of unity, however, can be attributed to the fact that DDRX was not complete until somewhat greater strains (Fig. 2a).

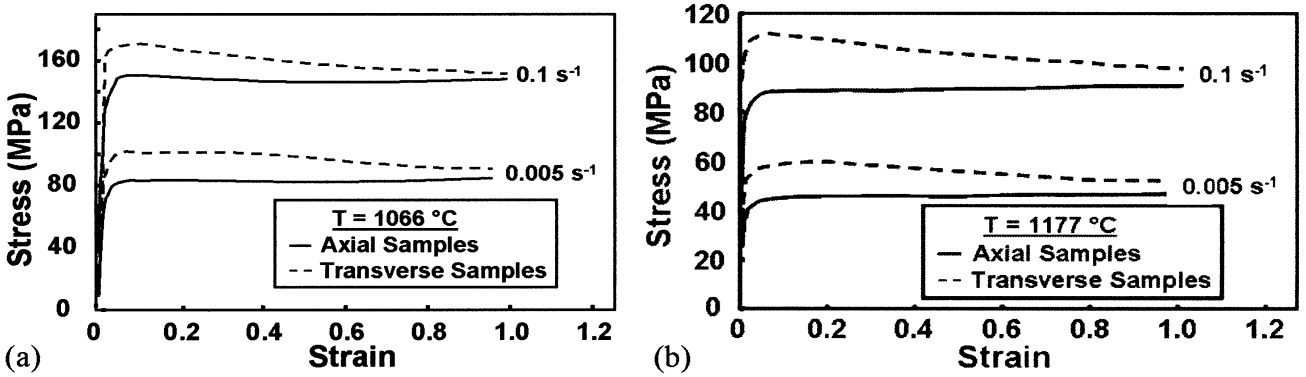

Fig. 1. True stress-strain curves for Waspaloy ingot material deformed at strain rates of 0.005 or 0.1 s^{-1} and test temperatures of (a) 1066°C or (b) 1177°C.

Dynamic Recrystallization Kinetics and Mechanisms – Monotonic Tests. DDRX kinetics in terms of recrystallized volume fraction as a function of strain (Fig. 2a) showed some scatter due to the non-uniformity of deformation in coarse, columnar-grain materials (discussed below). Nevertheless, a marked anisotropy (with respect to deformation direction relative to the columnar-grain orientation) was also found for the DDRX kinetics. In particular, the recrystallization rate was most rapid for samples in which the grains were oriented 45° to the compression direction and slowest in samples deformed parallel to the columnar-grain (axial) direction.

The DDRX observations were interpreted in terms of the orientation dependence of the average Taylor factor M_T. For a given imposed (macroscopic) strain increment $d\varepsilon$, the increment in internal work, which drives recrystallization, is $\tau d\gamma$, in which τ and $d\gamma$ denote the critical resolved shear stress and the sum of the (internal) shear strains, respectively. Because $M = d\gamma/d\varepsilon$, the internal work increment is equal to $\tau M d\varepsilon$. Assuming a fixed value of τ irrespective of test orientation, the

recrystallized volume fraction results were thus replotted as a function of Mε with M = 2.45, 3.1, and 3.55 for axial, transverse, and 45° samples (Fig. 2b). When plotted in this manner, the test-direction dependence of DDRX was greatly reduced. However, the complexity of deformation and the nature of nucleation (discussed next) in textured, ingot materials suggest that such a finding may be fortuitous. Other factors that affect the orientation dependence of recrystallization are briefly reviewed in the Discussion section below.

Despite large differences in grain-size and hence sites for grain-boundary nucleation of recrystallization, the strains required for DDRX of the Waspaloy *ingot* material were only somewhat larger than those previously measured for fine-grain, *wrought* Waspaloy [9] (Fig. 2a). This behavior was explained qualitatively on the basis of the nucleation of recrystallization within grain interiors due to the large carbide particles in Waspaloy ingot material (Fig. 3a) in addition to grain-boundary nucleation. Detailed metallographic characterization revealed, however, that classical grain-boundary (necklace) recrystallization, which is common in fine-grain, wrought superalloys (and other fcc metals with low stacking-fault energy), was *not* observed for the coarse, columnar-grain Waspaloy material. Rather, DDRX was somewhat non-uniform (Fig. 3b). EBSD analysis suggested the observed boundary-nucleated recrystallized grains lay principally along non-special, high-angle boundaries (Table 1) and hence that low-angle and special boundaries had low mobility.

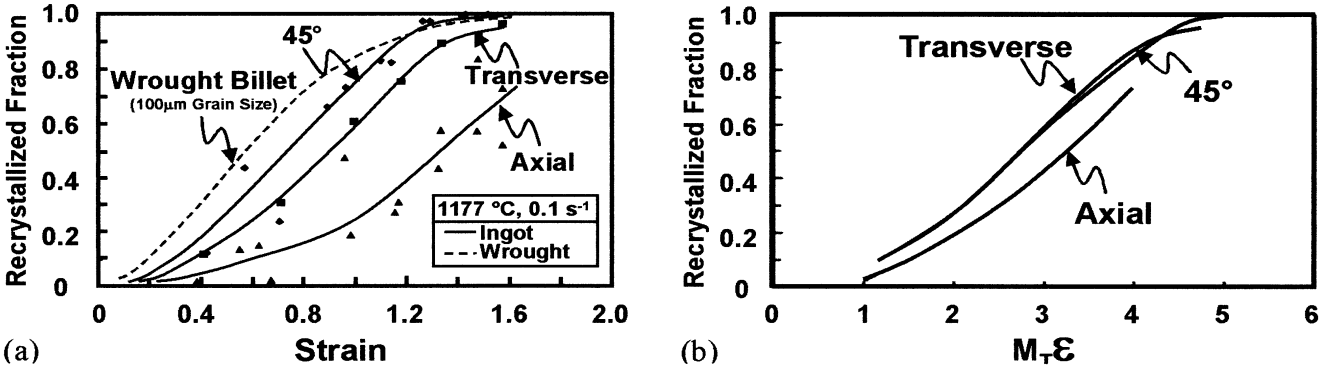

Fig. 2. Dependence of dynamic recrystallization kinetics on test orientation relative to the columnar-grain axis for cast-and-homogenized Waspaloy deformed at 1177°C and a strain rate of 0.1 s^{-1}: (a) DDRX kinetics as a function of imposed strain ε and (b) DDRX kinetics as a function of Mε. In (a), the behavior for the cast material is compared to results for wrought Waspaloy with a 100-μm grain size reported by Shen, et al. [9] (broken line).

Table 1. EBSD Measurements of Misorientation for Grain Boundaries in Fig. 3b

Grain Pair	Misorientation (Degrees)	Boundary Type*
1 & 2	56.2	High-angle boundary
2 & 3	57.5	High-angle boundary
2 & 4	3.8	Low-angle boundary
2 & 5	36.9	Σ5
2 & 6	24.9	Near Σ13a (22.62°)
4 & 5	40.5	Near Σ29a (43.61°)
5 & 6	45.7	Near Σ29a (43.61°)

*Tilt axis = <100>

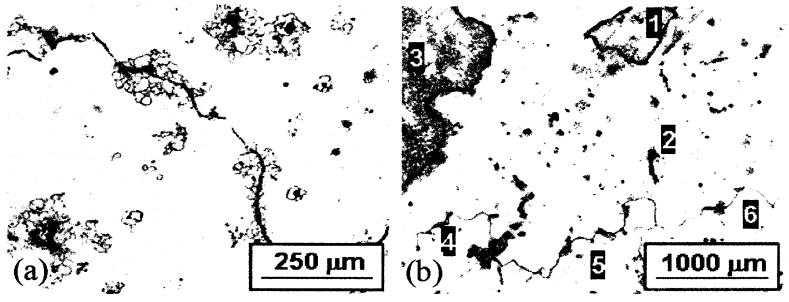

Fig. 3. Typical microstructures developed during hot compression of axially-oriented, Waspaloy-ingot double cone samples at 1066°C, 0.1 s^{-1}, and a local effective strain of ~1.5, illustrating (a) particle-stimulated and grain-boundary nucleation of DDRX and (b) the non-uniformity of DDRX. The numbers in (b) refer to grain orientations analyzed via EBSD (Table 1).

Dynamic Recrystallization Kinetics – Multi-Hit Tests. Despite the scatter associated with sampling statistics, the recrystallization behavior in the multi-hit tests on the coarse-grain ingot material also exhibited dependences on strain and test orientation similar to those found for monotonic tests (Figure 4). However, there were a number of significant differences. First, the overall kinetics were more rapid with respect to strain for the multi-hit tests (Figure 4a), most likely due to metadynamic/static recrystallization between increments of deformation. The similarity in behavior for the 30 and 60 second dwell-time results suggests that *metadynamic* recrystallization, which occurs during the first few seconds following deformation [9], is predominant. Such an enhancement led to recrystallization rates comparable to those observed during *dynamic* recrystallization of fine-grain wrought material [9], as shown in Figure 4b. Second, recrystallization in the multi-hit tests appeared to begin (due to particle-stimulated nucleation (PSN) at carbides) at a strain (~0.3 - 0.4), which was essentially the same for all three test orientations (Fig. 4b), unlike the observations for the monotonic tests (Fig. 2a). Last, the specific orientation dependence of the kinetics was less for the multi-hit tests compared to the monotonic tests (Figs. 2a, 4b).

Recrystallized grain sizes from the multi-hit experiments on the cast-and-homogenized Waspaloy ingot material, in which samples were quenched immediately after the final increment of deformation, were comparable to the dynamically recrystallized grain sizes from the corresponding monotonic tests. This suggests that boundary migration is relatively slow under the rapidly-decreasing driving-force conditions characterizing metadynamic recrystallization.

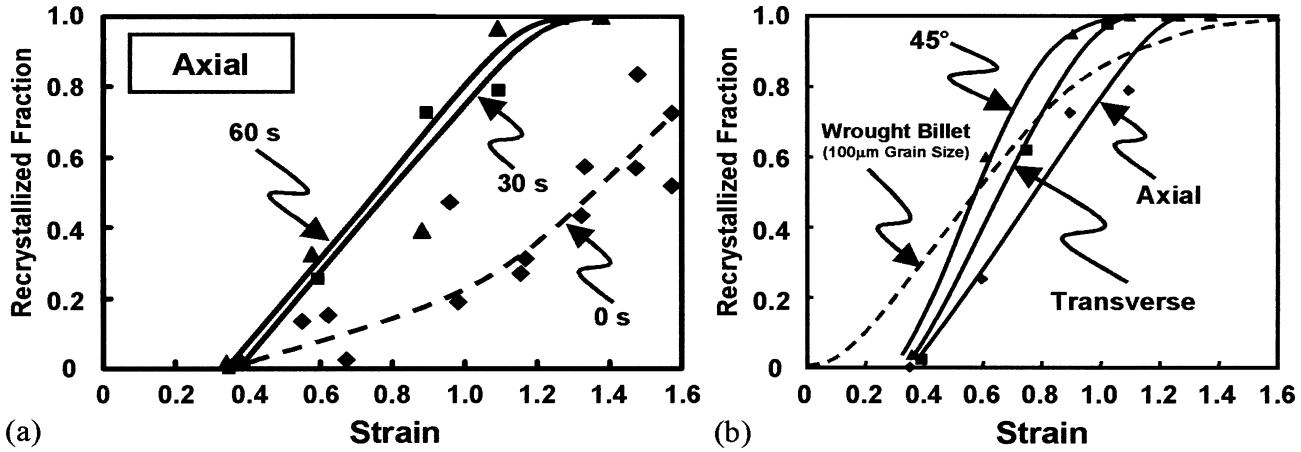

Fig. 4. Dependence of recrystallization kinetics on (a) dwell time (for axial samples) and (b) test orientation (for a 30-s dwell time) in Waspaloy ingot material deformed at 1177°C and $0.1s^{-1}$ using the multi-hit approach. The multi-hit results in (b) are compared to those for monotonically-deformed wrought Waspaloy with a 100-μm grain size reported by Shen, et al. [9] (broken line).

Discussion

The development of a suite of modeling tools has been begun to interpret (and predict) microstructure evolution during the hot working of superalloy ingots. These tools include cellular-automata, mesoscale-micromechanical, and crystal-plasticity-FEM models. Progress in these efforts is summarized in this section.

Cellular-Automata Model. A cellular-automata (CA) model is under development to predict recrystallized volume fractions, grain size distributions, and 'as large as' (ALA) grains in textured, columnar-grain superalloys during hot working at supersolvus temperatures. The model is designed to treat both DDRX and MDRX and is based on previous work [10-12] which focused on dislocation generation, recovery, and recrystallization in *isotropic* materials. The current version is

being enhanced to describe grain-boundary migration in terms of specified mobility and calculated driving forces as well as the influence of grain orientation/misorientation on dislocation generation and boundary mobility.

The CA model utilizes a uniform 490x490 (2D) lattice of 1-μm square cells to which several variables are assigned, i.e., dislocation density, orientation (Euler angles), and recrystallization state. The evolution of these variables with time is controlled by either deterministic rules or probabilistic methods.

For *dynamic recrystallization*, the simulation consists of (1) creation of a starting microstructure, (2) strain hardening and dynamic recovery, (3) nucleation of recrystallization at grain boundaries cells or second-phase particles, and (4) growth of DDRX grains. The starting polycrystalline microstructure is created through homogeneous, site saturated nucleation of randomly chosen cells. The orientation (and hence associated Taylor factor, assuming axisymmetric deformation) is chosen randomly. Nuclei for the starting structure then grow until impingement, transferring their orientations and Taylor factors to cells swept by the grain boundary. Strain hardening and dynamic recovery are implemented using the Laasraoui-and-Jonas equation [13],

$$d\rho_i = (U - \Omega\rho_{i-1})(\dot{\varepsilon})dt \quad (1)$$

in which ρ is the dislocation density, U is the hardening rate, Ω is the recovery variable, $\dot{\varepsilon}$ is strain rate, and dt is the time step. Furthermore, the hardening and recovery rates in Equation (1) are assumed to depend on crystallographic orientation through the Taylor factor (M_T).

Recrystallization nuclei are able to form at grain-boundary cells if the dislocation density is greater than a critical nucleation density and the probability is less than a certain value [14]. The critical dislocation density for nucleation, ρ_{CR}, is assumed to be some fraction of the steady-state density from Equation (1), viz., $\rho_{SS} = U/\Omega$. The orientation (and hence Taylor factor) of the nucleus are chosen randomly.

Following nucleation, the boundary velocity, v, is calculated as the product of the grain-boundary mobility, M, and driving force, P. The mobility is taken to be a function of the boundary misorientation and temperature T, i.e.,

$$M(\theta, T) = M_O(\theta)[\exp(-Q_M/RT)] \quad (2)$$

in which M_O is a pre-exponential term, and Q_M is the activation energy. The term M_O is assumed to increase exponentially with θ for low-angle boundaries ($\theta < 15°$) and be constant for high-angle boundaries ($\theta \geq 15°$) except for special boundaries deduced to have very small mobility (Table 1, Figure 5). The driving force P is estimated from the relation

$$P = (0.5Gb^2)(\rho_{NB} - \rho_C) \quad (3)$$

in which G is the shear modulus, b is the Burgers vector, ρ_C is the density in the grain boundary cell upon recrystallization (*initially* equal to zero, but subsequently undergoing strain hardening and dynamic recovery), and ρ_{NB} is the average density in those neighborhood cells which are part of the adjacent grain.

Metadynamic recrystallization is assumed to occur during the static dwell periods after deformation. As a static process, dislocation generation and dynamic recovery are assumed to be zero. Nucleation is possible, but less likely due to the lack of dislocation generation. Hence, the primary process assumed to occur during MDRX is the growth of nuclei formed during the preceding deformation. In the initial work reported here, static recovery has been assumed to be slow and hence not included.

The CA model successfully reproduced a number of the features of the DDRX and MDRX for Waspaloy ingot material. For example, CA predictions (assuming a fixed boundary mobility) qualitatively mirrored the noticeable increase in experimentally-observed DDRX kinetics due to the combined influence of heterogeneous nucleation at grain boundaries *and* homogeneous nucleation

associated with PSN (Figure 6a) [12]. Moreover, predicted Avrami exponents for nucleation solely at grain boundaries were 1.5 ± 0.3, while those for boundaries + PSN were 2-3 (Fig. 6b). These values are consistent with measurements.

The CA model also gave insight into MDRX during multi-hit deformation and the corresponding evolution of the average Taylor factor. Typical results for two-hit deformation of wrought Waspaloy at 1093°C, for example, revealed the importance of MDRX in comparison to DDRX (Figure 7a). With the assumed mobility behavior (Figure 5), the CA model predictions showed in addition that some degree of recrystallization texture should form and that the average Taylor would differ *slightly* from the typical value for an isotropic fcc material deformed under axisymmetric conditions (3.06). This finding contrasts with the frequent assumption that a perfectly random texture is formed, but is consistent with the experimental observations. In particular, the results showed that the average Taylor factor decreased during DDRX, increased during MDRX, and then decreased again during DDRX (Figure 7b).

Mesoscale, Mechanism-Based Model. The CA approach can be used to simulate microstructure evolution very well on a relatively small scale, but cannot be applied at every node of a finite-element mesh for a finite-size billet/workpiece due to computation limitations. On the other hand, phenomenological techniques (such as that based on the Avrami formulation) often lack the sophistication required to treat complex problems involving strain rate and temperature transients. Hence, an intermediate (meso-) scale, mechanism-based model for microstructure evolution has been developed [15]. Based on so-called meso-structural units (MSUs), the geometric description of microstructure in this model relies on several assumptions in terms of grain shape (spherical vs ellipsoidal) and the location of nucleation sites (near existing grain boundaries or inside the initial

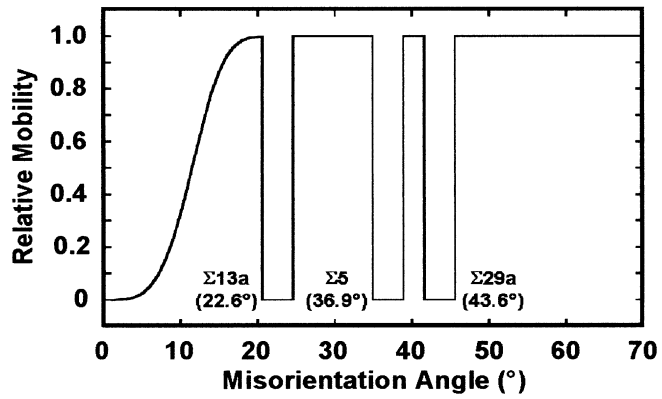

Fig. 5. Relative mobility of grain boundaries as a function of misorientation angle.

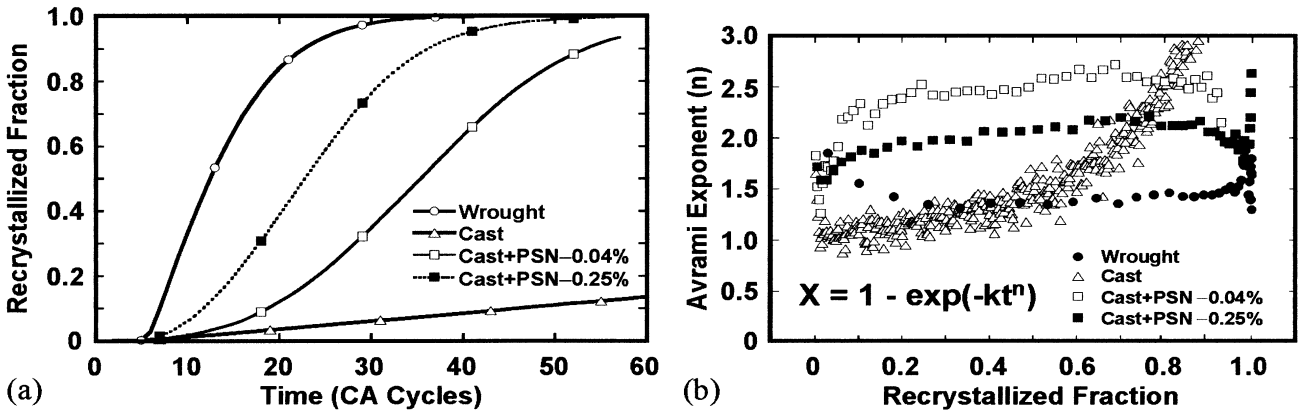

Fig. 6. CA predictions for DDRX with PSN of a material with various volume fractions of nucleating particles [12]: (a) Recrystallized fraction as a function of strain and (b) Avrami exponents.

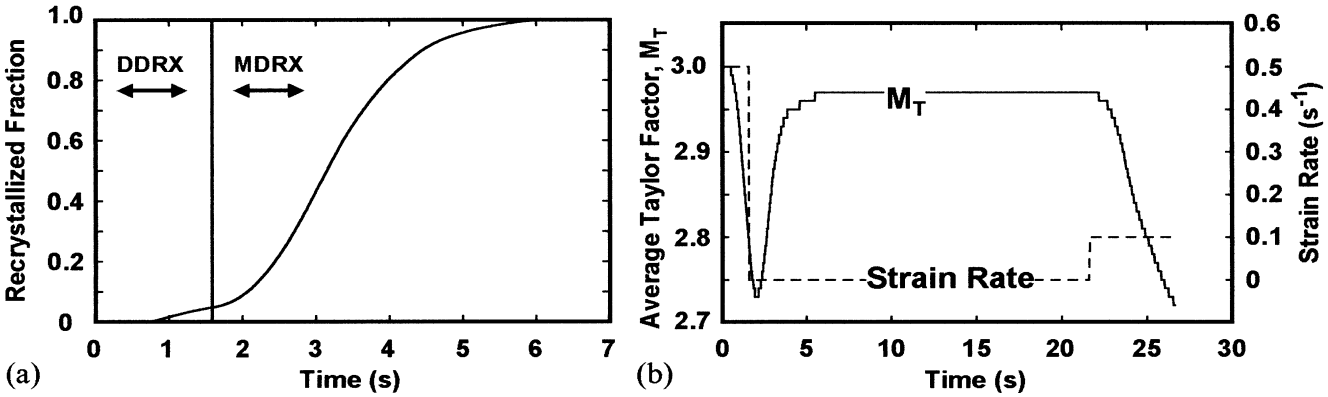

Fig. 7. Cellular-automata predictions of the temporal variation of (a) recrystallized fraction and (b) average Taylor factor during the double-hit deformation of wrought Waspaloy at 1093°C, 0.5 and 0.1 s^{-1} with a 20-s dwell between hits.

grains, as in PSN). Geometric relations deduced from these assumptions – mostly statistical expectancies of the surface of contact between grains – constrain the geometric variables of MSUs (grain size, grain density) into a framework that evolves in response to two kinds of inputs: nucleation rates and grain boundary velocities. From these inputs, the geometric framework allows the autonomous and internally-consistent calculation of the geometric evolution of the various grain populations during their growth-related interactions. A few variables are added to each MSU to quantify dislocation density, sub-boundary density/misorientation, or intrinsic properties such as its Taylor factor. Driving-force equations are used to evaluate the evolution of these variables and to deduce from them the required inputs of the geometric framework. The most important of these equations describe the dislocation mean free path (strain hardening), dynamic and metadynamic recovery, sub-boundary generation rate, the kinetics of sub-boundary disorientation, nuclei size, grain boundary mobility and velocity, etc. The mesoscale model combines advantages of both the CA and Avrami approaches in that the coefficients of its equations are physically based, as in the former approach, and very fast computation is possible due to the simplified geometric representation and averaging over the grain population each MSU represents, as for the latter approach. Details on the mesoscale model can be found in Reference 15.

The geometric framework was tested initially in the present work using simple input laws. For example, to establish the effect of strain rate on recrystallization, the influence of nucleation and grain-boundary migration velocity on recrystallization kinetics was evaluated (Figure 8a). At high strain rates, recrystallization was affected more by nucleation than boundary migration because there is relatively little time for migration to operate. Conversely, boundary migration accounts for most of the progression of recrystallization at low strain rates, during which oscillations in the flow curve may occur due to successive, synchronized waves of DDRX. The corresponding Avrami exponents varied from 1 to 3 depending primarily on the balance between nucleation and grain-boundary migration (i.e., strain rate) and secondly on the evolution of grain-boundary velocity during deformation, which is determined by the efficiency of dynamic recovery in reducing the driving force associated with stored dislocations. Other hypothetical simulations pertinent to the case involving both boundary nucleation and PSN showed that the latter increases both the recrystallization rate (Figure 8b) and the Avrami exponent, in broad agreement with observations for Waspaloy and CA simulations discussed above. Such behavior is a result of the increase of the total surface area between recrystallized and initial grains when intragranular recrystallized areas develop due to PSN. However, the density of PSN sites that was found to give rise to realistic recrystallization rates in the

simulations (10 to 100 particles per mm^3) was *lower* than the measured particle density in Waspaloy ingot material (i.e., ~1000 particles per mm^3 for a 0.25% fraction). This finding was rationalized on the basis of an observed particle-clustering effect in the Waspaloy-ingot material and the resulting impingement of intragranular islands of PSN recrystallization, thus giving rise to an effectively lower particle density.

Material coefficients for the driving-force equations were derived for Waspaloy in both the cast and the wrought conditions by fitting the recrystallization observations during monotonic and multi-hit deformation. Using this single set of coefficients, the average error in the predicted recrystallized fraction in both the dynamic and metadynamic regimes of *wrought* material (in comparison to the data of Shen, et al. [9]) was ~7.3 pct. (Figure 9). Model predictions for the *dynamic* recrystallization of the *ingot* microstructure (assuming a 2-3 s dwell prior to quenching) exhibited a similar accuracy. However, the *metadynamic* recrystallization behavior of ingot material (for hold times of 30s to 2h) exhibited a larger discrepancy (Figure 9), possibly due to insufficient sampling statistics or texture effects. In this regard, the magnitude of the difference between predicted and measured values of the recrystallized fraction for the ingot material seemed to depend on the test orientation. Ingot microstructures deformed in uniaxial compression with the columnar grains parallel to the compression axis showed a small discrepancy, only slightly greater than the one observed for wrought microstructures. In this case, all of the grains had the same Taylor factor, and thus the development of the deformation substructure around particles would be the same in each grain. Because recrystallization due to particle-stimulated nucleation predominates once it begins, the overall behavior is therefore not affected greatly by grain-boundary character. On the other hand, the Taylor factor in samples compressed along a direction lying 45° to the columnar-grain direction varied from grain-to-grain, reaching values as high as 3.66. In this case, strain incompatibility appears to be a major factor in the nucleation process through its effect on the development of crystallographic-orientation gradients, both near grain boundaries (due to the interaction of neighboring grains) and around particles that disturb the deformation field. Future crystal-plasticity FEM calculations can thus be expected to provide valuable information to enable an improved treatment of the effect of local texture/boundary misorientation on the critical strain for nucleation.

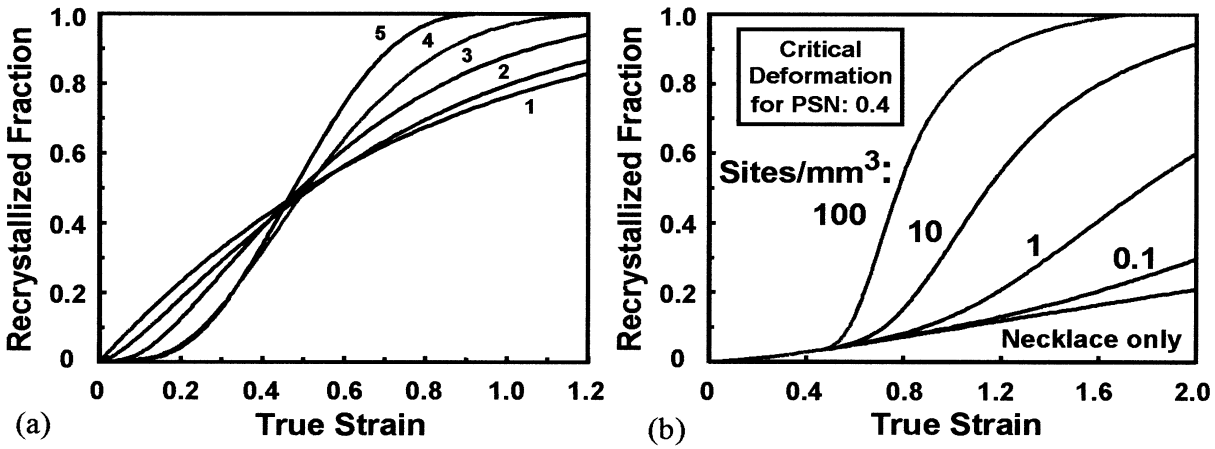

Fig. 8. Mesoscale model results for dynamic recrystallization kinetics: (a) Plot illustrating the competition between nucleation and grain-boundary migration in determining overall kinetics and (b) the effect of PSN on kinetics. In (a), the nucleation rates were 1 nucleus per 2.5 μm^2 (1), 10 μm^2 (2), or 100 μm^2 (3-5) of grain boundary and per unit strain; and the grain-boundary velocities were 0 μm (1), 25 μm (2), 45 μm (3), up to 80 μm (4), and up to 180 μm (5) per unit strain. In (b), the nucleation rate was 1 nucleus per 100 μm^2 of grain boundary and unit strain, and the grain boundary velocity was 100 μm per strain unit.

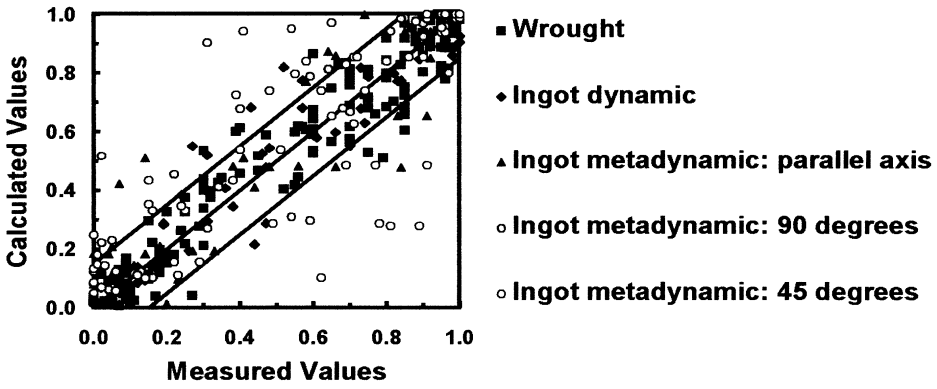

Fig. 9. Comparison of measured and predicted values of recrystallized fraction for coarse-grain, ingot and fine-grain, wrought conditions of Waspaloy.

Crystal-Plasticity FEM. The cellular automata and mechanism-base, mesoscale models rely on the accurate description of deformation fields. Unfortunately, the hot deformation of coarse, columnar-grain microstructures is not uniform at the grain scale. For example, the presence of non-uniformity is suggested by variations in recrystallization (Figure 10) that may mirror the variation in stored energy imparted during hot deformation. Hence, it is necessary to obtain a quantitative description of deformation heterogeneities within each grain as well as from one grain to another in order to better quantify those factors that influence both nucleation and growth during recrystallization processes.

Initial crystal-plasticity FEM simulations have sought to provide some insight into this challenge. Specifically, the variation of internal shear strains (γ) developed in the various grains of a transverse, columnar-grain sample during compression has been quantified for an imposed deformation consisting of either axisymmetric flow or uniaxial compression (Figure 11). The results reveal the very large difference in strain for grains of a given orientation (i.e., a specified orientation of the [001] axis relative to the compression direction), particularly for the axisymmetric case. Such variations underscore the important interactions of adjacent grains on plastic flow and strain non-uniformity. Additional experiments on transverse samples whose precise textures have been measured *prior* to deformation and accompanying crystal-plasticity FEM simulations are now in progress.

Future crystal-plasticity work (and accompanying experimental EBSD measurements) will also focus on the local deformation around carbide particles during hot working of ingot microstructures and thus provide insight into the particle-stimulated nucleation of dynamic recrystallization in such materials. The usefulness of such an effort can be inferred from related, prior work by Humphreys, Becker, and their co-workers [1, 16, 17] dealing with polyslip deformation during the channel-die compression of aluminum and aluminum-silicon single crystals. In this work, experimental results and corresponding crystal-plasticity models revealed that the average (maximum) misorientation between subgrains/grains formed in the deformation zone around coarse particles (of a size of the order of 10 μm) and the matrix was given by the expression θ_{max} (degrees) = $40\{\varepsilon/(1+\varepsilon)\}$, in which ε denotes the imposed strain. For a strain of 0.4, at which PSN was observed during the hot working of the Waspaloy ingot, the maximum misorientation would thus be approximately 11 degrees. For this misorientation, a subgrain boundary would begin to have adequate mobility for the PSN nucleus to migrate. Humphreys and Hatherly [1] also suggested a criterion for the growth of PSN nuclei into the surrounding matrix. Assuming that the average radius of curvature of the nucleus is *twice* that of the particle, this criterion is $d_g \geq 4\gamma_b/\rho Gb^2$, in which d_g denotes the particle diameter (10 μm in the present work), γ_b is the boundary energy (taken to be ~0.4 J/m^2), ρ is the matrix dislocation density,

G is the shear modulus (4.8 x 10^{10} N/m^2 for Waspaloy at T~1100°C [18]), and b is the burgers vector length (~2.5 x 10^{-10} m). Inverting this relation, the matrix dislocation density for nucleus growth can thus be estimated to be ~5.4 x 10^{13} m^{-2}. This value is comparable to that deduced previously from the analysis of the supersolvus kinetics of dynamic and metadynamic recrystallization of coarse and fine grain Waspaloy, i.e. ~3 x 10^{13} m^{-2} [19].

Fig. 10. Microstructure developed in a double-cone sample of Waspaloy ingot material upset to a 2:1 reduction at 1066°C, 0.1 s^{-1} and then held at temperature for 30 min. prior to water quenching. The FEM-predicted local strain for the region shown was 0.6.

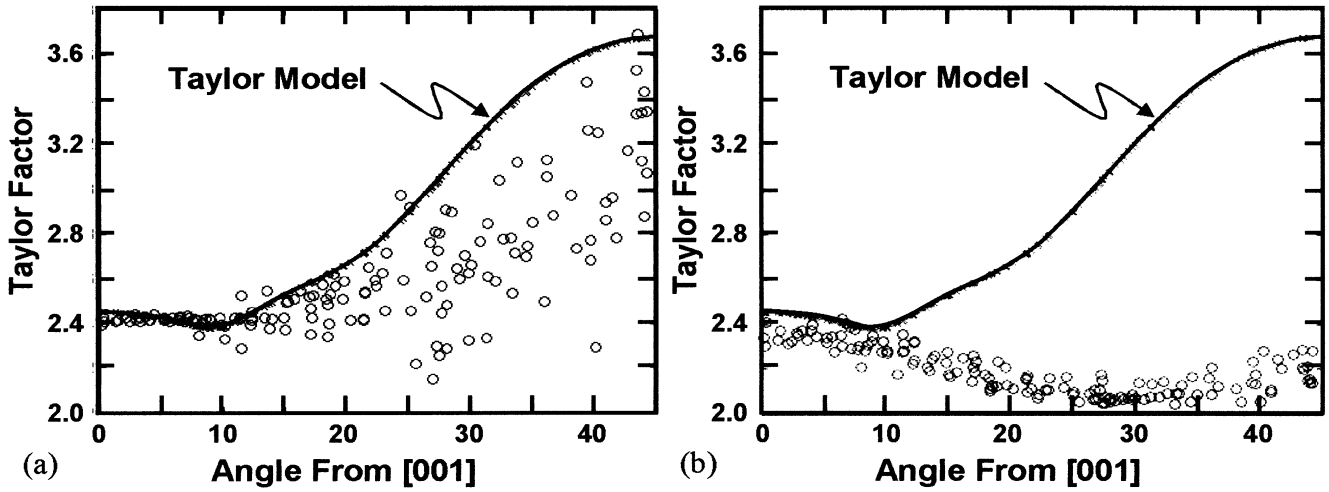

Fig. 11. Crystal-plasticity FEM predictions of the local Taylor factor ($d\gamma/d\varepsilon$) in various grains of a transverse hot-compression sample of Waspaloy ingot material subjected to (a) axisymmetric compression or (b) uniaxial compression. The model results are compared to Taylor (isostrain) model predictions, which are indicated by the continuous curve in each plot. The [010] fiber axis lay in the transverse direction; the abscissae on the plots denote the angle between the compression direction and the [001] direction.

Summary and Conclusions

The breakdown of coarse, columnar-grain ingots of nickel-base superalloys consists of a complex thermomechanical process in which field variables (strain, strain rate, temperature, interpass dwell time), texture, and second-phase particles are all important. Uniaxial and double-cone hot compression tests under both monotonic (uninterrupted) and multi-hit conditions have shown that

the overall strains required for recrystallization of a typical superalloy (Waspaloy) are comparable to those for the corresponding wrought material. These observations can be explained on the basis of the PSN in addition to boundary nucleation as well as metadynamic recrystallization (during multi-hit processes). Cellular automata and mechanism-based, mesoscale models have been successful in replicating many of the observed features of the recrystallization process at least qualitatively and, in some cases, quantitatively. In the future, refined analyses incorporating deformation heterogeneity will provide additional input to obtain a more complete description of microstructure evolution during the processing of superalloy ingots.

Acknowledgements- This work was conducted as part of the in-house research activities of the Metals Processing Group of the Air Force Research Laboratory's Materials and Manufacturing Directorate. The support and encouragement of the Laboratory management and the Air Force Office of Scientific Research (Dr. J.S. Tiley, program manager) are gratefully acknowledged. Technical discussions with Professor F. Montheillet (Ecole des Mines de Saint-Etienne) and the yeoman assistance of P.N. Fagin in conducting the experimental work are also much appreciated. Two of the authors were supported through Air Force Contracts FA8650-04-D-5235 (RLG) and F33615-03-D-5801 (JPT).

References

[1] F.J. Humphreys and M. Hatherly: *Recrystallization and Related Annealing Phenomena* (Elsevier Science Ltd., Oxford, UK, 1996).

[2] M.G. Glavicic, P.A. Kobryn, F. Spadafora and S.L. Semiatin: Mater. Sci. Eng. A Vol. A346 (2003), p. 8

[3] C.M. Sellars: Mater. Sci. Techn. Vol. 6 (1990), p. 1072

[4] C. Devedas, I.V. Samarasekera and E.B. Hawbolt: Metall. Trans. A Vol. 22A (1991) p. 335.

[5] M. Avrami: J. Chem. Phys. Vol. 8 (1940), p. 212.

[6] S.L. Semiatin, D.S. Weaver, P.N. Fagin, M.G. Glavicic, R.L. Goetz, N.D. Frey, R.C. Kramb and M.M. Antony : Metall. Mater. Trans. A Vol. 35A (2004), p. 679

[7] S.L. Semiatin, P.N. Fagin, M.G. Glavicic and D. Raabe: Scripta Mater. Vol. 50 (2004), p. 625

[8] G.Y. Chin and W.L. Mammel : Trans. TMS-AIME Vol. 239 (1967), p. 1400

[9] G. Shen, S.L. Semiatin, and R. Shivpuri: Metall. Mater. Trans. A Vol. 26A (1995), p. 1795

[10] R.L. Goetz and V. Seetharaman: Scripta Mater. Vol. 38 (1998), p. 405

[11] R.L. Goetz and V. Seetharaman: Metall. Mater. Trans. A Vol. 29A (1998), p. 2307

[12] R.L. Goetz: Scripta Mater. Vol. 52 (2005), p. 851

[13] A. Laasraoui and J.J. Jonas: Metall. Trans. A Vol. 22A (1991), p. 1545

[14] G. Kugler and R. Turk: Acta Metall. Vol. 52 (2004), p. 4659

[15] J.P. Thomas, F. Montheillet, and S.L. Semiatin: submitted to Metall. Mater. Trans. A (2006).

[16] R. Becker, J.F. Butler, Jr., H. Hu and L.A. Lalli: Metall. Trans. A Vol. 22A (1991) p. 45

[17] F.J. Humphreys and M.G. Ardakani: Acta Metall. Mater. Vol. 42 (1994) p. 749

[18] R.F. Wilde and N.J. Grant: ASTM Proceedings Vol. 57 (1957) p. 917

[19] J.P. Thomas and S.L. Semiatin: *Proc. MS&T '06* (TMS, Warrandale, PA, 2006), in press.